A Novel 3D UAV Channel Model for A2G Communication Environments Using AoD and AoA Estimation Algorithms

Hao Jiang, *Member, IEEE*, Zaichen Zhang, *Senior Member, IEEE*, Cheng-Xiang Wang, *Fellow, IEEE*, Jiangfan Zhang, *Member, IEEE*, Jian Dang, *Member, IEEE*, Liang Wu, *Member, IEEE*, and Hongming Zhang, *Member, IEEE*

***Abstract*— In this article, we propose a three-dimensional (3D) multi-input multi-output (MIMO) channel model for air-to-ground (A2G) communications in unmanned aerial vehicles (UAV) environments, where the UAV transmitter and ground receiver are in motion in the air and on the ground, respectively. A novel angular estimation algorithm is proposed to estimate the real-time azimuth angle of departure (AAoD), elevation angle of departure (EAoD), azimuth angle of arrival (AAoA), and elevation angle of arrival (EAoA) based on the non-stationary nature of the channel model. In the model, we investigate the time-varying spatial cross-correlation functions (CCFs) and temporal auto-correlation functions (ACFs) with respect to the different moving directions and velocities of the UAV transmitter and ground receiver. Furthermore, we derive and study the Doppler power spectral densities (PSDs) and power delay profiles (PDPs) of the proposed channel model. Numerical results show that characteristics of the proposed channel model are very close to those of practical measurements, which provide a new and practical approach to evaluate the performance of next generation UAV-MIMO communication systems.**

***Index Terms*— UAV channel model, A2G communication environments, angular estimation algorithm, non-stationarity, channel characteristics.**

Manuscript received October 10, 2019; revised February 21, 2020 and May 8, 2020; accepted July 19, 2020. Date of publication July 24, 2020; date of current version November 18, 2020. This work was supported by the National Key R&D Program of China under grant 2018YFB1801101, the National Natural Science Foundation of China (NSFC) (No. 61771248, 61960206006, 61971136, 61960206005, 61871111, and 61501109), Frontiers Science Center for Mobile Information Communication and Security, the High Level Innovation and Entrepreneurial Research Team Program in Jiangsu, the High Level Innovation and Entrepreneurial Talent Introduction Program in Jiangsu, the Research Fund of National Mobile Communications Research Laboratory, Southeast University, under Grant 2020B01, the Fundamental Research Funds for the Central Universities under grant 2242019R30001, the Huawei Cooperation Project, the EU H2020 RISE TESTBED2 project under Grant 872172, the Major Program of the Natural Science Foundation of Institution of Higher Education of Jiangsu Province (No.14KJA510001), Zhejiang Lab (No. 2019LC0AB02), Open Research Fund of National Mobile Communications Research Laboratory, Southeast University (No. 2020D14), and Cynthia Tang endowment in Computer Engineering, Missouri University of Science and Technology, Rolla, MO, USA. The associate editor coordinating the review of this article and approving it for publication was R. Zhang. *(Corresponding author: Zaichen Zhang.)*

Hao Jiang is with the College of Artificial Intelligence, Nanjing University of Information Science and Technology, Nanjing 210044, China, and also with the National Mobile Communications Research Laboratory, Southeast University, Nanjing 210096, China (e-mail: jianghao@nuist.edu.cn).

Zaichen Zhang and Cheng-Xiang Wang are with the National Mobile Communications Research Laboratory, Southeast University, Nanjing 210096, China, and also with the Purple Mountain Laboratories, Nanjing 211111, China (e-mail: zczhang@seu.edu.cn; chxwang@seu.edu.cn).

Jiangfan Zhang is with the Department of the Electrical and Computer Engineering, Missouri University of Science and Technology, Rolla, MO 65409 USA (e-mail: jiangfanzhang@mst.edu).

Jian Dang and Liang Wu are with the National Mobile Communications Research Laboratory, Southeast University, Nanjing 210096, China (e-mail: dangjian@seu.edu.cn; wuliang@seu.edu.cn.)

Hongming Zhang is with the Software Engineering, Beijing University of Posts and Telecommunications, Beijing 100876, China (e-mail: zhanghm@bupt.edu.cn).

Color versions of one or more of the figures in this article are available online at http://ieeexplore.ieee.org.

Digital Object Identifier 10.1109/TCOMM.2020.3011716

I. Introduction

A. Motivation

UNMANNED aerial vehicles (UAVs), also known as "drones", are expected to be deployed in air-to-ground (A2G) communications for traffic monitoring, disaster recovery, and military reconnaissance [1], [2]. The recent existing literature has introduced a variety of fifth generation (5G) and beyond 5G (B5G) technologies into A2G communication systems [3], [4]. Reliable knowledge of realistic propagation channel models, which provide an effective way to approximately express the propagation characteristics between the transmitters and receivers, serves as the foundation for designing and evaluating the performance of UAV communication systems [5]. This motivates us to study the channel characteristics of A2G communications in UAV environments.

B. Related Work

Generally, channel models are broadly categorized into stochastic and deterministic models, e.g., models using the ray-tracing method that requires a detailed description of a specific communication scenario. It is worth mentioning that stochastic models, which rely on large numbers of measurements that contain the underlying statistical properties of wireless channels, are able to describe a variety of communication scenarios by properly setting model parameters. The existing works suggested various geometry-based stochastic channel models (GBSMs) to simulate the distribution of interfering objects in wireless communication environments [6], [7]. As the mobility of UAV transmitters are high and the

moving directions are arbitrary in real UAV communication environments, it is reasonable to adopt a three-dimensional (3D) channel model to describe the distribution of interfering objects in A2G communication scenarios [10]. The authors in [11] and [12] applied the 3D geometry-based multi-input multi-output (MIMO) channel models to characterize the A2G communications in UAV environments, with an assumption that the propagation components from the UAV transmitter to the mobile receiver (MR) experience single interaction. In the models, the authors used cylinders to describe the UAV propagation environments for A2G communications. Furthermore, authors in [13] and [14] developed GBSMs with 3D angular parameters to describe the scattering environments for A2G communications. In addition, the authors in [15] provided a 3D elliptic-cylinder model to describe the propagation environments around the UAV and MR in A2G communication scenarios, which can be further used for the performance evaluation of UAV wireless communication systems. The authors in [16] proposed a 3D single-cylindrical ring stochastic model for MIMO wideband non-stationary channels between the UAV and ground user. Based on the reference model, some important channel characteristics were derived and investigated. In [17], the authors proposed a 3D non-stationary two-cylinder stochastic model, as well as the corresponding deterministic and simulation models for non-isotropic UAV-MIMO Ricean fading channels. Furthermore, in [18], Cheng *et al.* proposed a non-geometrical stochastic model (NGSM) for non-stationary wideband vehicular communication channels. However, we should notice that the interfering objects, which mainly represent the moving airships, birds, etc., are randomly scattered between UAV transmitters and ground receivers in real and dynamic A2G communication scenarios. In overall, the above solution of geometry-based channel modeling is insufficient to reflect the A2G communications in UAV environments.

To fill the above gaps, several studies [19]–[21] developed cluster-based stochastic channel models to investigate the propagation properties in complex wireless communication environments, where the interfering objects are randomly distributed over the network. More specifically, Li *et al.* [19] provided a cluster-based channel model for vehicle-to-vehicle (V2V) communications, which introduced the von Mises distribution to describe the 3D angular parameters of the propagation links both in the horizontal and vertical planes, as well as an exponential distribution to reflect the propagation distances from the transmitter and receiver to the cluster. In [20], the authors proposed a 3D non-stationary wideband twin-cluster channel model as well as the corresponding simulation model for MIMO communication systems. In the model, the authors assumed that the angular parameters and propagation distances follow wrapped Gaussian and exponential distributions, respectively. Ghazal *et al.* [21] developed a non-stationary MIMO channel model to investigate the time variation of the wireless communication environments by introducing time-varying angular parameters, i.e., the angle of departure (AoD) and angle of arrival (AoA). Nevertheless, it is worth mentioning that the model parameters in non-stationary channels continuously vary over time as the motion of the transmitter and receiver is ongoing. Based on the model parameters of the motion of the transmitter and receiver, we can derive the closed-form expressions of the time-varying AoD and AoA statistics in wireless non-stationary channels. It is worth mentioning that the interfering objects in UAV communication scenarios are randomly distributed in the 3D space and the propagation environments are dynamic; therefore, the classic distributions (i.e., Gaussian or exponential distributions) fails to characterize the transmit/receive distances and angular parameters in wireless channels. This motivates us to propose an efficient estimation algorithm to determine the angular parameters and propagation path lengths in UAV channels. Nonetheless, we argue that the above method can be further adopted to effectively evaluation the performance of UAV wireless communication systems [22].

To evaluate the performance of wireless communication systems efficiently, a variety of angular estimation algorithms have been proposed in the literature. Specifically, the authors in [23] proposed Rayleigh fading channel models in space-, time-, and frequency-domain. Simulation results demonstrate that these models are able to effectively characterize the performance of discrete-time MIMO communication systems. Later, Xiao *et al.* [24] introduced an estimation algorithm into a Clarke's model, the results demonstrated that the algorithm could be used to reduce the variation of temporal correlations of a fading realization. To reduce the dimensionality of the measurement matrix for angular estimation, a pre-estimation algorithm is introduced in [25]. Furthermore, in massive MIMO communication systems, Huang *et al.* [26] developed a deep learning-based scheme for achieving super-resolution angular estimation in wireless channels. Moreover, the authors in [27] and [28] proposed channel estimation models for MIMO communication systems based on the known model parameters. However, it is worth mentioning that when we characterize the propagation properties in real wireless communication environments, it is important to introduce an angular estimation algorithm with low complexity and high accuracy into wireless channel models.

C. Main Contributions

In this work, a novel 3D MIMO channel model is proposed to describe the A2G communications in UAV environments, as shown in Fig. 1, where the UAV transmitter and ground receiver are in motion in the air and on the ground, respectively. The main contributions of this article are summarized as follows:

- We propose a computationally efficient solution to estimate the real-time azimuth angle of departure (AAoD), elevation angle of departure (EAoD), azimuth angle of arrival (AAoA), and elevation angle of arrival (EAoA) in the proposed channel model. To be specific, we first estimate the angular parameters in the preliminary stage before the UAV transmitter and ground receiver move. Then, the real-time AAoD/EAoD and AAoA/EAoA are efficiently estimated based on the estimated initial angular parameters and the motion parameters of the UAV and MR. It is worth mentioning that the proposed

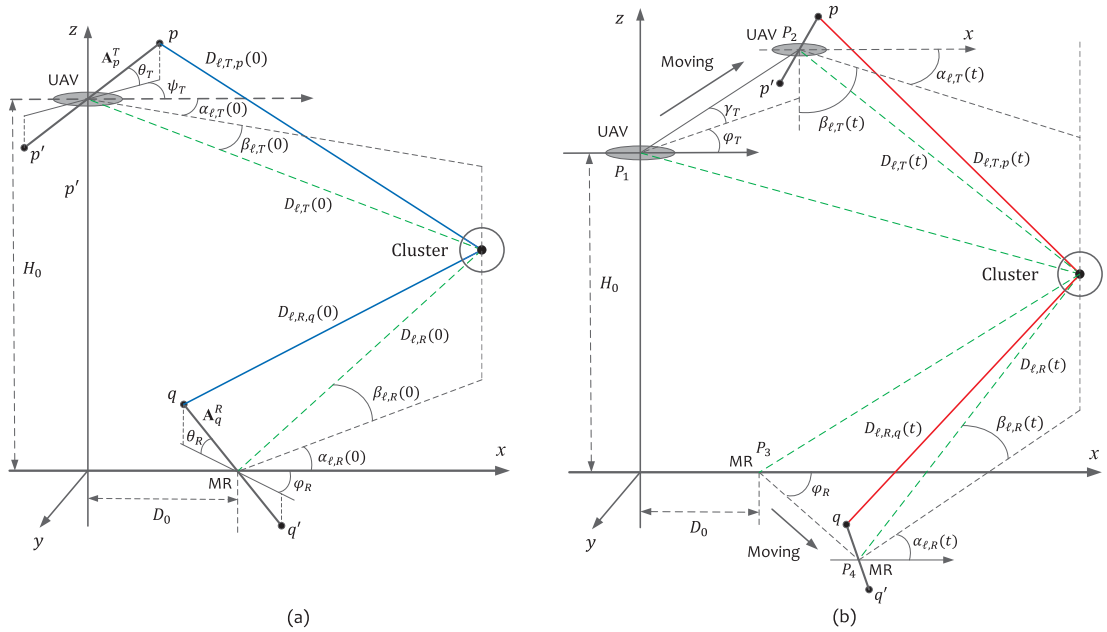

Fig. 1. Proposed 3D MIMO channel model for A2G communications in UAV environments. (a) In the preliminary stage; (b) In the real-time stage.

algorithm can be extended to the applications of other communication scenarios, which provides a new and practical approach to evaluate the performance of next-generation wireless communication systems.

- In the proposed channel model, we investigate the propagation properties for different moving directions and velocities of the UAV transmitter in the air and the receiver on the ground level. The time-varying spatial cross-correlation functions (CCFs) and temporal auto-correlation functions ACFs) with respect to the different moving time are investigated. Furthermore, the Doppler power spectral densities (PSDs) and power delay profiles (PDPs) of the proposed model are derived and thoroughly studied.
- The time-varying AAoD/EAoD and AAoA/EAoA estimations are derived to capture the non-stationarity of the proposed channel model. Furthermore, the impacts of the moving directions and velocities on the time-varying channel characteristics are compared with those of practical channel measurements. The results show that the proposed channel characteristics fit the measurements in realistic A2G communication scenarios very well.

The remainder of this article is organized as follows. Section II presents the general system channel model. In Section III, the complex channel impulse responses (CIRs) of the UAV-MIMO channel model are estimated. Section IV provides the underlying characteristics of the proposed UAV-MIMO channel model, and then numerical results and discussions are given in Section V. Finally, our conclusions are given in Section VI.

II. Channel Model

In this section, we propose a novel 3D MIMO channel model for A2G communications in UAV environments, where the UAV transmitter and the ground receiver are equipped with M_T and M_R uniform linear array (ULA) antenna arrays [29], as shown in Fig. 1. In the preliminary stage, which corresponds to the condition when the UAV transmitter and ground receiver are static, we define the line connecting the center of the ground receiver and the projection point of the center of the UAV in the horizontal plane as the x-axis, which remains unchanged even when the UAV and MR are in motion. Let us define $\alpha_{\ell,T}$ and $\beta_{\ell,T}$ as the AAoD and EAoD of the waves that impinge on the ℓ-th cluster, respectively; while $\alpha_{\ell,R}$ and $\beta_{\ell,R}$ as the AAoA and EAoA of the waves traveling from the ℓ-th cluster, respectively. It is worth mentioning that the waves emerge from the UAV to the MR are easily blocked by tree crowns or buildings in complicated A2G communication environments, and therefore the line-of-sight (LoS) propagation components are extremely weak when compared with the non-LoS (NLoS) components in the signal received at the ground receiver [13]. In view of this, we assume that the obstacles in the proposed A2G channel model are static near to the MR, while the UAV moves in the air is high enough to be free of scattering environments.

As shown in Fig. 1, we define δ_T and δ_R as the spacing between two adjacent UAV transmit and ground receive antenna elements, respectively. The orientations of the transmit antenna array relative to the x-axis and to the azimuth plane are denoted as ψ_T and θ_T, respectively. Similarly, at the MR, the orientations of the antenna array relative to the x-axis and to the azimuth plane are denoted as ψ_R and θ_R, respectively. Here, parameters ψ_T, θ_T, ψ_R, and θ_R are all set to be constant. The physical properties of the proposed MIMO channel can be described by a matrix $\mathbf{H}(t) = \left[h_{pq}(t,\tau)\right]_{M_R \times M_T}$ of size $M_R \times M_T$, where $h_{pq}(t,\tau)$ represents the complex CIR between the p-th ($p = 1, 2, \ldots, M_T$) transmit antenna and q-th ($q = 1, 2, \ldots, M_R$) receive

antenna, i.e., [30]

$$h_{pq}(t,\tau) = \sum_{\ell=1}^{L(t)} h_{\ell,pq}(t)\ \delta\big(\tau - \tau_\ell(t)\ \big), \tag{1}$$

where $h_{\ell,pq}(t)$ represents a narrowband process where all the propagation components have the same delay $\tau_\ell(t)$, $L(t)$ denotes the number of the propagation paths. Here, it is worth mentioning that the delay $\tau_\ell(t)$ of the waves emerging from the UAV to the MR is time-variant because of the motion of the UAV and MR. Therefore, the complex fading envelope $h_{\ell,pq}(t)$ can be expressed as

$$\begin{aligned} h_{\ell,pq}(t) \ &= \omega_\ell e^{j\left(\varphi_0 - 2\pi f_c \tau_{\ell,pq}(t)\ \right)} \\ &\quad \times e^{j\frac{2\pi}{\lambda} v_T t \cos\left(\alpha_{\ell,T} - \varphi_T\right)\cos\left(\beta_{\ell,T} - \gamma_T\right)} \\ &\quad \times e^{j\frac{2\pi}{\lambda} v_R t \cos\left(\alpha_{\ell,R} - \varphi_R\right)\cos\beta_{\ell,R}}, \end{aligned} \tag{2}$$

where $\tau_{\ell,pq}(t)$ represents the propagation delay of the waves emerging from the p-th transmit antenna to the q-th receive antenna via the scatterers within the ℓ-th cluster, f_c denotes the carrier frequency, ω_ℓ is the attenuation factors, and λ is the carrier wavelength. Parameters v_T, v_R, φ_T, γ_T, and φ_R are set to be constant. Specifically, v_T and v_R are the moving velocities of the UAV and MR, respectively, φ_T and γ_T are the UAV's moving directions in the horizontal and vertical planes, respectively, φ_R is the MR's moving direction in the horizontal plane. Moreover, the transmit and receive antenna spacing elements are not obvious when compared to the propagation path lengths; therefore, it is unnecessary to define the AAoD/EAoD and AAoA/EAoA for the different antenna elements [31]. To proceed further with a stochastic description of the statistical channel model in (2), it is of vital importance to introduce a random variable for the model parameters. Here, we should mention that the proposed 3D channel model is stochastic, which is mainly suitable for A2G communications in different UAV environments by adjusting the certain parameters. This is mainly due to the fact that the random phase φ_0 of the complex fading envelope $h_{\ell,pq}(t)$ is assumed to have a uniform distribution in the interval from $-\pi$ to π, i.e., $\varphi_0 \sim [-\pi, \pi)$. Therefore, the matrix $\mathbf{H}(t) = \big[h_{pq}(t,\tau)\big]_{M_R \times M_T}$, which characterizes the physical properties of our UAV-MIMO channel model, is stochastic.

III. Estimation of the Complex CIRs

A. Algorithm Description

As shown in Figs. 1(a) and 1(b), when the UAV transmitter moves from position P_1 to P_2, and the MR moves from position P_3 to P_4, the channel model varies over time; and therefore the complex CIRs for different moving time t should be updated to characterize the time-varying properties of the channel model [32]. However, it seems impossible to estimate the complex CIRs in a real-time manner due to the high computational complexity of the estimation process. To address the above issue, let us assume that the MR is able to receive the signal transmitted from the UAV for a while in the preliminary stage of the system, which corresponds to the time period before the UAV and MR move, i.e., $t = 0$. Then, we propose a three-step approach to estimate the real-time channel information of the proposed model, which can be shown as follows:

- First, we propose an approach to estimate the initial AAoD/EAoD and AAoA/EAoA, which means the proposed channel model during the initialization before the UAV and MR move can be estimated;
- Next, for every time instant when the UAV and MR are in motion, we estimate the real-time AAoD/EAoD and AAoA/EAoA based on the estimated initial angular parameters and the motion parameters of the UAV and MR;
- Finally, by substituting the estimates of the time-varying AAoD/EAoD and AAoA/EAoA into the complex CIRs in (1), the complex CIRs of the proposed UAV-MIMO channel model in a real-time manner can be obtained.

In this article, we adopt the maximum likelihood estimation (MLE) to obtain the coarse AAoD/EAoD and AAoA/EAoA estimations. The purpose of the angle estimation is for channel modeling. The MLE is an asymptotically optimal estimator which generally performs very well even though the number of observation is not large. It is worth mentioning that the waves emitted from the UAV experience the multi-paths impinging on the scatterers within the cluster before reaching the MR. In this case, we assume that every scatterer within the cluster approximately has the same propagation distance from the center of the corresponding antenna array, and moves with the same velocity. A similar assumption was made in [33]. Therefore, we consider the same AAoD/EAoD and AAoA/EAoA to characterize the multi-paths propagation from the transmit/receive antennas to the scatterers within the cluster.

B. AAoD/EAoD and AAoA/EAoA Estimations in the Real-Time Stage

Based on the estimated angular parameters in the preliminary stage discussed in the Appendix, as well as the motion parameters of the UAV transmitter and ground receiver, we can estimate the real-time AAoD/EAoD and AAoA/EAoA in the proposed UAV-MIMO channel model. Note that when the UAV and receiver are in motion, i.e., $t \neq 0$, the closed-form expressions of the path lengths and angular parameters are time-variant. In this stage, the complex fading envelope $h_{\ell,pq}(t)$ can be expressed as

$$h_{\ell,pq}(t) \ = \omega_\ell e^{j\left(\varphi_0 - 2\pi f_c \tau_{\ell,pq}(t)\ \right)} \times e^{j2\pi t f_{\ell,pq}(t)}, \tag{3}$$

In the proposed channel model, the distance vectors from the centers of the transmit and receive antenna arrays to the ℓ-th cluster during the initialization can be expressed as

$$\mathbf{D}_{\ell,T}(0) = D_{\ell,T}(0) \begin{bmatrix} \cos\beta_{\ell,T}(0)\cos\alpha_{\ell,T}(0) \\ \cos\beta_{\ell,T}(0)\sin\alpha_{\ell,T}(0) \\ \sin\beta_{\ell,T}(0) \end{bmatrix} \tag{4}$$

$$\mathbf{D}_{\ell,R}(0) = D_{\ell,R}(0) \begin{bmatrix} \cos\beta_{\ell,R}(0)\cos\alpha_{\ell,R}(0) \\ \cos\beta_{\ell,R}(0)\sin\alpha_{\ell,R}(0) \\ \sin\beta_{\ell,R}(0) \end{bmatrix}, \tag{5}$$

where $\alpha_{\ell,T}(0)$, $\beta_{\ell,T}(0)$, $\alpha_{\ell,R}(0)$, and $\beta_{\ell,R}(0)$ are, respectively, the AAoD, EAoD, AAoA, and EAoA of the waves via the scatterers within the ℓ-th cluster in the preliminary stage, i.e., $t = 0$. It is worth mentioning that these angular parameters can be estimated by the solution in the Appendix. Note again that the MR is in motion with the speed v_R and direction φ_R in the azimuth plane, while the UAV transmitter is in motion in the 3D space with speed v_T and directions φ_T and γ_T for the horizontal and vertical planes, respectively. Therefore, the transmit and receive velocity vectors, denoted by $\mathbf{v}_T$ and $\mathbf{v}_R$, respectively, can be expressed as

$$\mathbf{v}_T = v_T \begin{bmatrix} \cos\gamma_T \cos\varphi_T \\ \cos\gamma_T \sin\varphi_T \\ \sin\gamma_T \end{bmatrix}, \tag{6}$$

$$\mathbf{v}_R = v_R \begin{bmatrix} \cos\varphi_R \\ \sin\varphi_R \\ 0 \end{bmatrix}, \tag{7}$$

Consequently, the distance vectors from the transmit and receive antennas to the ℓ-th cluster in real-time stage can be expressed as

$$\mathbf{D}_{\ell,T}(t) = \mathbf{D}_{\ell,T}(0) - \mathbf{v}_T t, \tag{8}$$

$$\mathbf{D}_{\ell,R}(t) = \mathbf{D}_{\ell,R}(0) - \mathbf{v}_R t. \tag{9}$$

Accordingly, the real-time distance vectors from the p-th transmit antenna and the q-th receive antenna to the ℓ-th cluster, denoted by $\mathbf{D}_{\ell,T,p}(t)$ and $\mathbf{D}_{\ell,R,q}(t)$, respectively, can be computed as

$$\mathbf{D}_{\ell,T,p}(t) = \mathbf{D}_{\ell,T}(t) - \mathbf{A}_{T,p}, \tag{10}$$

$$\mathbf{D}_{\ell,R,q}(t) = \mathbf{D}_{\ell,R}(t) - \mathbf{A}_{R,q}, \tag{11}$$

where $\mathbf{A}_{T,p}$ and $\mathbf{A}_{R,q}$ denote the distance vector from the center points of the MT and MR arrays to the p-th transmit antenna and the q-th receive antenna, respectively, which can be expressed as

$$\mathbf{A}_{T,p} = \frac{M_T - 2p + 1}{2}\delta_T \begin{bmatrix} \cos\theta_T \cos\psi_T \\ \cos\theta_T \sin\psi_T \\ \sin\theta_T \end{bmatrix} \tag{12}$$

$$\mathbf{A}_{R,q} = \frac{M_R - 2q + 1}{2}\delta_R \begin{bmatrix} \cos\theta_R \cos\psi_R \\ \cos\theta_R \sin\psi_R \\ \sin\theta_R \end{bmatrix}. \tag{13}$$

Furthermore, in (3), $\tau_{\ell,pq}(t) = (D_{\ell,T,p}(t) + D_{\ell,R,q}(t))/c$, where $D_{\ell,T,p}(t)$ and $D_{\ell,R,q}(t)$ denote the propagation path lengths from the p-th transmit antenna and the q-th receive antenna to the ℓ-th cluster, which can be derived by taking the magnitude of $\mathbf{D}_{\ell,T,p}(t)$ and $\mathbf{D}_{\ell,R,q}(t)$, respectively. The c is the speed of light. Based on the above derivations, the Doppler frequency component of the ℓ-th propagation link between the p-th transmit antenna and q-th receive antenna can be expressed as

$$f_{\ell,pq}(t) = \frac{1}{\lambda}\Big(\frac{\langle \mathbf{D}_{\ell,T,p}(t), \mathbf{v}_T\rangle}{\big|\big|\mathbf{D}_{\ell,T,p}(t)\big|\big|} + \frac{\langle \mathbf{D}_{\ell,R,q}(t), \mathbf{v}_R\rangle}{\big|\big|\mathbf{D}_{\ell,R,q}(t)\big|\big|}\Big), \tag{14}$$

where $\langle\cdot\rangle$ represents the inner product. To characterize the non-stationarity of the proposed UAV-MIMO channel model, the time-varying closed-form expressions of the AAoD and EAoD are respectively shown in as

$$\alpha_{\ell,T}(t) = \arctan\frac{D_{\ell,T}(0)\cos\beta_{\ell,T}(0)\sin\alpha_{\ell,T}(0) - v_T t\cos\gamma_T\sin\varphi_T}{D_{\ell,T}(0)\cos\beta_{\ell,T}(0)\cos\alpha_{\ell,T}(0) - v_T t\cos\gamma_T\cos\varphi_T} \tag{15}$$

$$\begin{aligned}\beta_{\ell,T}(t) &= \operatorname{arccot}\Big\{\frac{1}{D_{\ell,T}(0)\sin\beta_{\ell,T}(0) - v_T t\sin\gamma_T} \\ &\quad\times\Big[\big(D_{\ell,T}(0)\cos\beta_{\ell,T}(0)\sin\alpha_{\ell,T}(0) - v_T t\cos\gamma_T\sin\varphi_T\big)^2 \\ &\quad+\big(D_{\ell,T}(0)\cos\beta_{\ell,T}(0)\cos\alpha_{\ell,T}(0) \\ &\quad- v_T t\cos\gamma_T\cos\varphi_T\big)^2\Big]^{1/2}\Big\}.\end{aligned} \tag{16}$$

Observe that the time-varying AAoA $\alpha_{\ell,T}(t)$ and EAoA $\beta_{\ell,T}(t)$ are closely related to the UAV and MR motion (i.e., direction, velocity, and time), the preliminary angular parameters ($\alpha_{\ell,T}(0)$ and $\beta_{\ell,T}(0)$), the LoS path length D_0 and the UAV's height H_0, as shown in Fig. 1. Similar as before, the time-varying expressions of the AAoA and EAoA can be respectively calculated as

$$\alpha_{\ell,R}(t) = \arctan\frac{D_{\ell,R}(0)\cos\beta_{\ell,R}(0)\sin\alpha_{\ell,R}(0) - v_R t\sin\varphi_R}{D_{\ell,R}(0)\cos\beta_{\ell,R}(0)\cos\alpha_{\ell,R}(0) - v_R t\cos\varphi_R} \tag{17}$$

$$\begin{aligned}\beta_{\ell,R}(t) &= \operatorname{arccot}\Big\{\frac{1}{D_{\ell,R}(0)\sin\beta_{\ell,R}(0)} \\ &\quad\times\Big[\big(D_{\ell,R}(0)\cos\beta_{\ell,R}(0)\sin\alpha_{\ell,R}(0) - v_R t\sin\varphi_R\big)^2 \\ &\quad+\big(D_{\ell,R}(0)\cos\beta_{\ell,R}(0)\cos\alpha_{\ell,R}(0) - v_R t\cos\varphi_R\big)^2\Big]^{1/2}\Big\}.\end{aligned} \tag{18}$$

Overall, the procedure for generating the proposed UAV-MIMO channel model is shown in Algorithm I at the left top of the next page.

It is worth mentioning that the proposed channel modeling solution is significantly different from the existing 3GPP like geometric based modeling methods. Specifically, the existing 3GPP channel models mainly assume that the channel information are known in advance [15]–[18], and then investigate the channel characteristics. However, in our channel model, we propose an approach to estimate the channel information during the initialization stage before the UAV and MR move. Then, we predict the real-time channel characteristics based on the UAV/MR motion (i.e., direction, velocity, and time) and the estimated initial parameters.

IV. Channel Characteristics of the Proposed Model

To demonstrate the rationality and generality of the proposed 3D UAV-MIMO channel model, it is necessary to derive and investigate the channel characteristics based on the above

Algorithm 1 Procedure for the Proposed Channel Generation

1: Generate the initial parameters, including the distance D_0 between the horizontal distance between the centers of the UAV and MR, as well as the UAV's height H_0;
2: Perform the proposed algorithm to estimate the angular parameters during the initialization before the UAV and MR move.
3: Compute the time-varying closed-form expressions of the AAoD $\alpha_{\ell,T}(t)$, EAoD $\beta_{\ell,T}(t)$, AAoA $\alpha_{\ell,R}(t)$, and EAoA $\beta_{\ell,R}(t)$ based on (15)-(18);
Then, the time-varying statistical properties of the UAV-MIMO channel model can be described;
4: Incorporate the time-varying geometric angular parameters and propagation paths into the complex fading envelope in (3), the expression of the $h_{\ell,pq}(t)$ can be derived.
5: By substituting the complex fading envelope $h_{\ell,pq}(t)$ into (1), the complex CIR between the p-th transmit antenna and q-th receive antenna can be obtained. Then, the proposed 3D UAV-MIMO channel model, which physical properties is characterized by the channel matrix $\mathbf{H}(t) = \left[h_{pq}(t,\tau)\right]_{M_R \times M_T}$, can be generated.

derived complex CIRs [4]. In the following part, we investigate the characteristics of the proposed channel model, including those of the spatial CCFs, temporal ACFs, Doppler PSDs, and PDPs.

A. Spatial CCFs

For the proposed UAV-MIMO communication system, the complex CIRs have the ability to characterize the channel effect [6]. Once calculated, the complex CIRs can be used to investigate the statistical properties of the communication system. In the proposed UAV-MIMO channel model, the spatial CCF between the propagation link from the p-th transmit antenna to q-th receive antenna and the link from the p'-th ($p' = 1, 2, , M_T$) transmit antenna to q'-th ($q' = 1, 2, , M_R$) receive antenna can be defined as the correlation between the fading envelopes $h_{\ell,pq}(t)$ and $h_{\ell,p'q'}(t)$, i.e., [34]

$$\rho_{h_{\ell,pq};h_{\ell,p'q'}}(t,\tau') = \mathbb{E}\Big[h_{\ell,pq}(t)\ h^*_{\ell,p'q'}(t-\tau')\Big], \quad (19)$$

where the expectation operation $\mathbb{E}[\cdot]$ applies only to the random phase φ_0, and $(\cdot)^*$ denotes the complex conjugate operation. By averaging over the random phases φ_0, the spatial CCFs of the proposed UAV-MIMO channel model can be expressed by substituting (2) into (19) as follows:

$$\begin{aligned}\rho_{h_{\ell,pq};h_{\ell,p'q'}}(t,\tau') = {} & e^{j\frac{2\pi}{\lambda}\left(tf_{\ell,pq}(t)-(t-\tau')f_{\ell,p'q'}(t-\tau')\right)} \\ & \times e^{-j2\pi f_c\left[D_{\ell,T,p}(t)+D_{\ell,R,q}(t)\right]/c} \\ & \times e^{j2\pi f_c\left[D_{\ell,T,p'}(t-\tau')+D_{\ell,R,q'}(t-\tau')\right]/c}.\end{aligned} \quad (20)$$

By substituting the closed-form expressions of the time-varying transmit and receive propagation path lengths into (20), we can obtain the spatial CCF of two different propagation components in the model.

B. Temporal ACFs

It is worth mentioning that the complex fading envelope of the proposed UAV-MIMO channel model in (2) have different physical properties at different moving time t; therefore, it is important to investigate the temporal ACF of the propagation link from the p-th transmit antenna to the q-th receive antenna at different time difference Δt, which can be expressed as

$$r_{\ell,pq}(t,\Delta t) = \mathbb{E}\Big[h_{\ell,pq}(t)h^*_{\ell,pq}(t+\Delta t)\Big]. \quad (21)$$

After applying similar techniques as introduced at the beginning of this section, we can show that the temporal ACF of the proposed model as

$$\begin{aligned}r_{\ell,pq}(t,\Delta t) = {} & e^{j\frac{2\pi}{\lambda}\left(tf_{\ell,pq}(t)-(t+\Delta t)f_{\ell,pq}(t+\Delta t)\right)} \\ & \times e^{-j2\pi f_c\left[D_{\ell,T,p}(t)+D_{\ell,R,q}(t)\right]/c} \\ & \times e^{j2\pi f_c\left[D_{\ell,T,p}(t+\Delta t)+D_{\ell,R,q}(t+\Delta t)\right]/c}.\end{aligned} \quad (22)$$

Obviously, we note that all the above investigated channel properties are time-variant on account of the non-stationary properties of the proposed model.

C. Doppler PSDs

In the proposed A2G channel, the received signal frequency constantly varies on account of the motion between the UAV transmitter and ground receiver. Here, when we take the Fourier transform of the temporal ACF $r_{\ell,pq}(t,\Delta t)$ in terms of the time difference Δt, we can obtain the Doppler PSD of the proposed model as

$$\begin{aligned}S_{\ell,pq}(t,f) = {} & \int_{-\infty}^{\infty} r_{\ell,pq}(t,\Delta t)e^{-j2\pi f\Delta t}\mathrm{d}\Delta t \\ = {} & \int_{-\infty}^{\infty} e^{j\frac{2\pi}{\lambda}\left(tf_{\ell,pq}(t)-(t+\Delta t)f_{\ell,pq}(t+\Delta t)\right)}e^{-j2\pi f\Delta t} \\ & \times e^{-j2\pi f_c\left[D_{\ell,T,p}(t)+D_{\ell,R,q}(t)\right]/c} \\ & \times e^{j2\pi f_c\left[D_{\ell,T,p}(t+\Delta t)+D_{\ell,R,q}(t+\Delta t)\right]/c}\mathrm{d}\Delta t.\end{aligned} \quad (23)$$

It is worth mentioning that the Doppler PSDs of the proposed model are determined by the moving directions (i.e., φ_T, γ_T, and φ_R), velocities (i.e., v_T and v_R), and time t of the UAV and MR.

D. PDPs

Based on the measurements of the spatial average of the proposed CIRs, we can obtain the closed-form expression of the proposed PDP, which can be used to characterize the intensity of a signal received through the proposed A2G channel [32]. In wideband V2V channels, the propagation delays are discrete, which are in correspondence with the propagation delays in different taps [31]. However, the delay $\tau_\ell(t)$ in the proposed UAV channel model is time-variant

because of the motion of the UAV and MR, and hence the propagation delay τ is continuous. Accordingly, the PDP of the proposed model can be calculated as

$$P_{h_{\ell,pq}}(t,\tau) = \left|h_{\ell,pq}(t,\tau)\right|^2 = \left|\omega_\ell e^{j\left(\varphi_0 - 2\pi f_c \tau_{\ell,pq}(t)\right)} e^{j\frac{2\pi}{\lambda} t f_{\ell,pq}(t)} \delta\left(\tau - \tau_\ell(t)\right)\right|^2. \quad (24)$$

Observe that the propagation delay $\tau_\ell(t)$, and the complex fading envelope $h_{\ell,pq}(t)$ are all dependent on the moving time t. Therefore, the proposed PDP is completely determined by the moving time t.

Note that the prior works on investigating the underlying channel characteristics, i.e., the spatial CCFs, temporal ACFs, Doppler PSDs, and PDPs, require accurate knowledge of model parameters. In practice, they are however difficult to obtain in real wireless communication scenarios. To address this issue, we propose a solution to estimate the AAoD/EAoD and AAoA/EAoA, which can be further used to estimate the channel parameters, i.e., propagation paths and angular parameters. Hence, the complex CIRs can be estimated to characterize the physical properties of wireless channels and improve the accuracy of the channel models for different wireless communication scenarios. The proposed algorithms provide an efficient solution to accurately acquire the UAV-MIMO channel characteristics, and can be further used for the B5G communication system design and simulations.

V. Numerical Results and Discussions

In this section, we evaluate the proposed estimation algorithm to estimate the AAoD/EAoD and AAoA/EAoA in the preliminary stage. Then, we study the statistical propagation properties of the proposed UAV-MIMO channel model.

A. Angular Parameters Estimations

Let us assume that the UAV transmitter and MR in the preliminary stage are static for a while. During this time period, the MR is able to receive the complete information from the transmitter. Here, the p-th transmitted signal is defined as a cosine signal, i.e., $x_p\left(kT - \tau_\ell(0)\right) = \cos\left(kT - \tau_\ell(0)\right)$. For the sake of generality, basic parameters in the following simulations are obtained using $f_c = 5.9$ GHz, $\omega_\ell = 10$, $\sigma^2 = 5$, $\psi_T = \psi_R = \pi/12$, $\theta_T = \theta_R = \pi/12$, $\lambda = 0.2$, and $M_T = M_R = 4$. The exact values of the angular parameters are set as $\alpha_{\ell,T}(0) = \pi/4$, $\beta_{\ell,T}(0) = -\pi/6$, $\alpha_{\ell,R}(0) = 2\pi/3$, and $\beta_{\ell,R}(0) = \pi/3$. The number of Monte Carlo iterations is set as 10000.

Based on the Newton-Raphson method, the performance of the MLE of the AAoD/EAoD and AAoA/EAoA estimations in preliminary stage is provided in Fig. 2. The MLE of angle estimation is defined as $\mathbb{E} = \left[|\nu_{\text{true}} - \nu_{\text{est}}|^2\right]$, with ν_{true} representing the exact angle in the proposed communication system, and ν_{est} is its estimated counterpart. It is seen from Fig. 2 and Fig. 3 that the estimation errors for estimating the AAoD/EAoD and AAoA/EAoA gradually decrease as the number of samples K increases, which demonstrates that

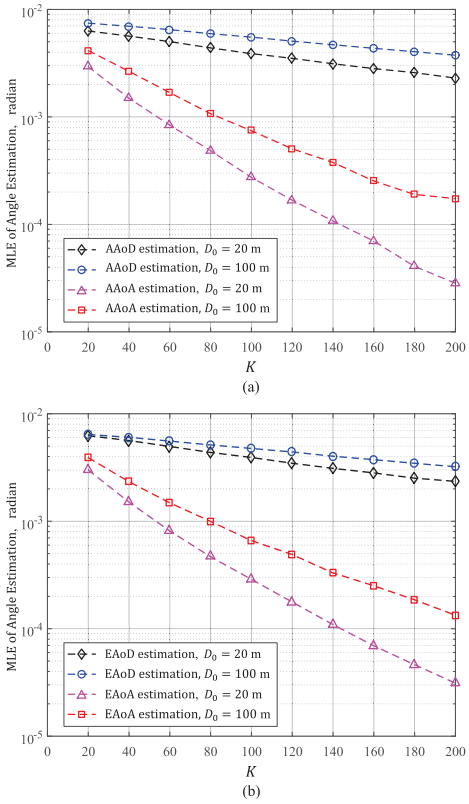

Fig. 2. Mean squared error performance in the preliminary stage before the UAV and MR move. (a) AAoD and AAoA estimation; (b) EAoD and EAoA estimation when $H_0 = 100$ m.

the estimation performance can be very good for channel modeling, especially when K is large [35]. Furthermore, we notice that when the horizontal distance D_0 between the centers of the UAV and MR increases from 20 m to 100 m, the MLEs of the angular estimations increase correspondingly.

To estimate the MLE performance of the real-time AAoD/AAoA and EAoD/EAoA in the proposed UAV-MIMO channel model, the moving parameters of the UAV and MR in Fig. 3 are set $\varphi_T = \pi/3$, $\gamma_T = \pi/3$, $\varphi_R = \pi/4$, $v_T = 5$ m/s, and $v_R = 20$ m/s. In the figure, we notice that the MLE at different time instants gradually decrease as the K increase, which is in correspondence with the results in Fig. 2. Furthermore, when the moving time t increases from 2 s to 30 s, the horizontal distance D_0 between the centers of the UAV and MR increases correspondingly; therefore, the MLE performance increases slowly.

B. Spatial CCFs and Temporal ACFs

It is worth mentioning that (20) plotting Fig. 4 is a Bessel function, which indeed fluctuates when increasing the antenna spacing but the general trend is to decrease with the increase of the antenna spacing. In our simulations, the initial parameter settings are somehow in agreement with the environments of channel measurements. The simulation results fit the measurements in [36] very well, which also demonstrates that the spatial CCFs of the wireless channel models gradually

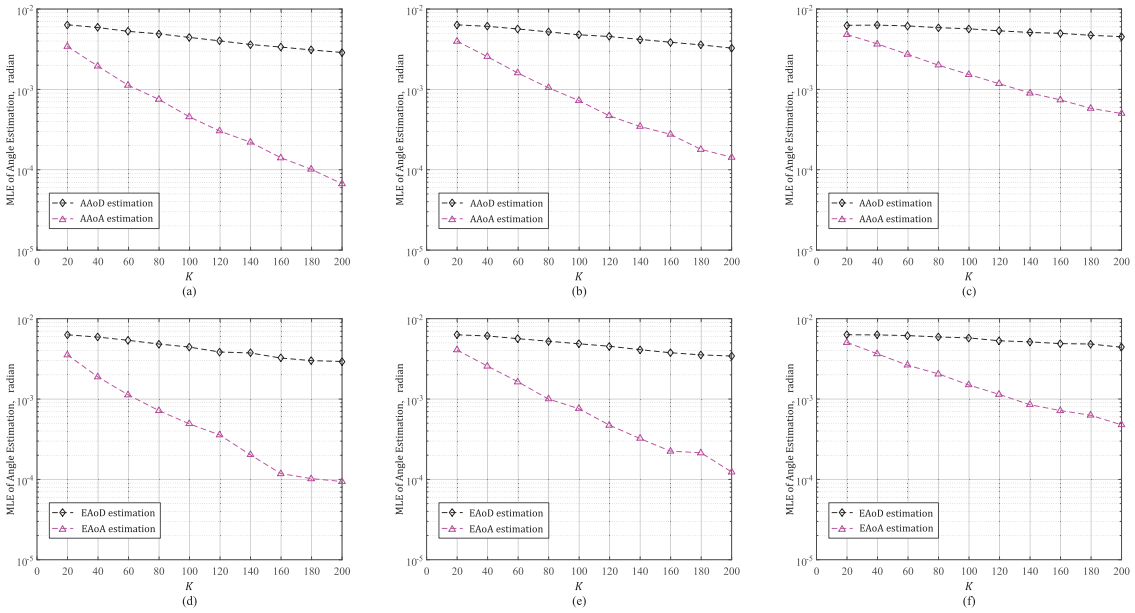

Fig. 3. Mean squared error performance in the real-time stage for different moving time of the UAV and MR when $H_0 = 100$ m and $D_0 = 50$ m. (a) $t = 2$ s; (b) $t = 10$ s; (c) $t = 30$ s; (d) $t = 2$ s; (e) $t = 10$ s; (f) $t = 30$ s.

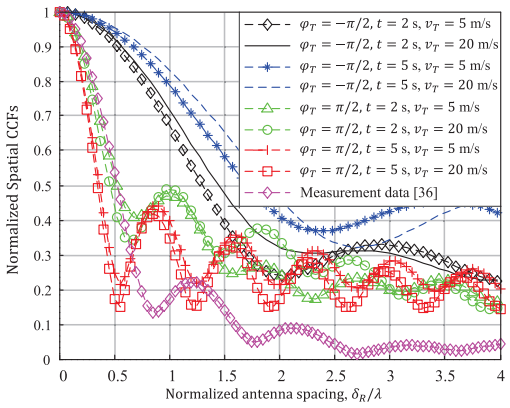

Fig. 4. Spatial CCFs of the proposed 3D channel model for different UAV's moving velocities and directions when $H_0 = 100$ m, $D_0 = 20$ m, $\gamma_T = 0$, and $v_R = 0$.

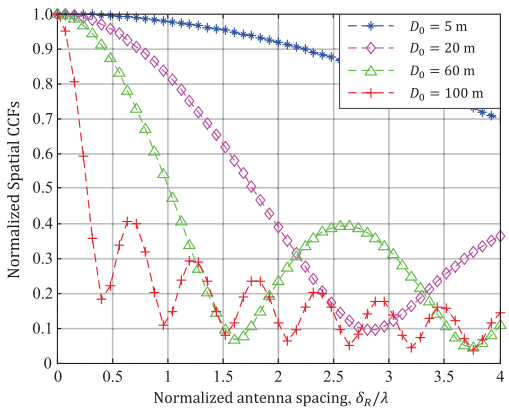

Fig. 5. Spatial CCFs of the proposed channel model for different horizontal distances between the centers of the UAV and MR when $H_0 = 100$ m and $v_T = v_R = 0$.

decrease as the adjacent spacing of the MR antenna array increases. It has been demonstrated in [15] that the UAV's moving direction has a substantial impact on the A2G channel characteristics. In light of this, we investigate the spatial CCFs of the proposed channel model for some specific UAV motion directions and velocities in Fig. 4. The figure shows that when the UAV moves towards the horizontal plane, i.e., $\varphi_T = 0$ and $\gamma_T = -\pi/2$, the spatial correlations gradually increase as the velocity of the UAV increases from 5 m/s to 20 m/s. However, when the UAV moves away from the horizontal plane, i.e., $\varphi_T = 0$ and $\gamma_T = \pi/2$, the correlations decrease as the UAV's velocity rises from 5 m/s to 20 m/s. Simulation results in Fig. 4 fit the conclusions in [16] very well, thereby demonstrating the accuracy of the above analysis and derivations. It is worth noting that the spatial correlation varies more heavily as the moving time t increases from 2 s to 5 s. In addition, in Fig. 5, the spatial CCFs of the proposed model are relatively large as the distance D_0 between the centers of the UAV and MR is smaller than 5 m. However, when the distance is larger than 100 m, the spatial CCFs of the proposed model decrease extremely fast. Therefore, we can conclude that the spatial CCFs of the proposed UAV channel model have different behaviors as the distance between the centers of the UAV and MR varies, which is in agreement with the results in [17].

It is stated in [1] that the flight altitude of the UAV ranges from a few meters to a few hundred meters; therefore, we investigate the spatial CCFs of the proposed channel model for different heights of the UAV in Fig. 6, to demonstrate the impact of the UAV's height on the channel characteristics. It can be observed that when the height of the UAV increases from 10 m to 200 m, the spatial correlation

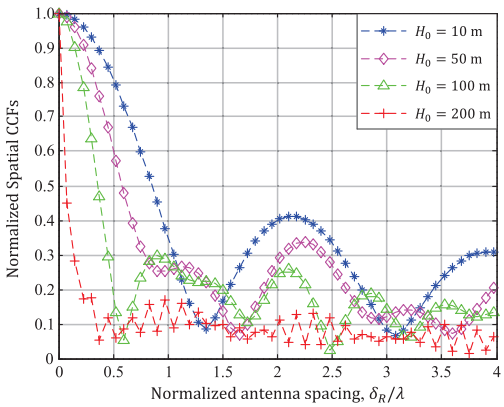

Fig. 6. Spatial CCFs of the proposed channel model for different heights of the UAV when $D_0 = 50$ m and $v_T = v_R = 0$.

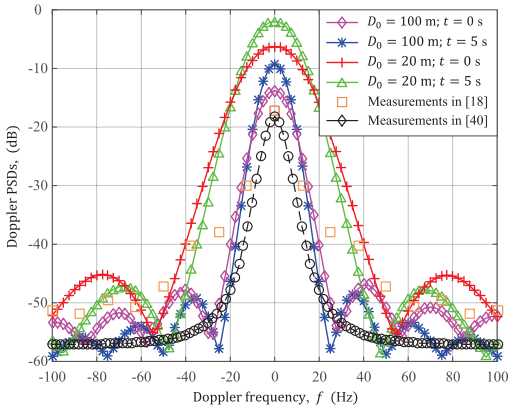

Fig. 8. Doppler PSDs of the proposed channel model for different distances D_0 and different MR's moving time t.

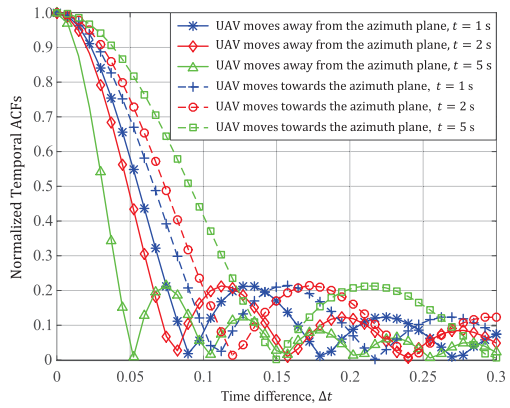

Fig. 7. Temporal ACFs of the proposed channel model for different UAV's moving directions and time when $H_0 = 100$ m, $D_0 = 20$ m, $v_R = 0$, and $v_T = 10$ m/s.

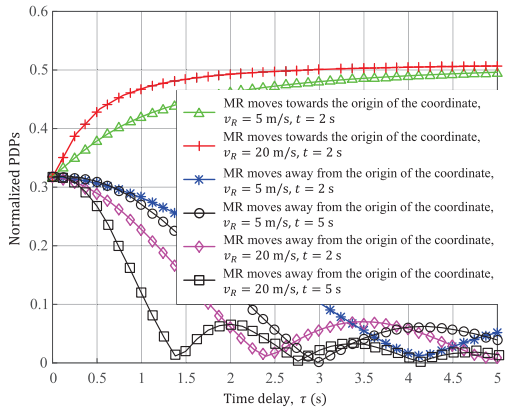

Fig. 9. PDPs of the proposed channel model for different MR's moving directions and velocities when $H_0 = 100$ m, $D_0 = 20$ m, and $v_T = 0$.

decreases gradually, which is in consistent with the simulation results in [15].

By using (21), Fig. 7 illustrates the temporal ACFs of the proposed channel model at three different moving time, i.e., $t = 1$ s, $t = 2$ s, and $t = 5$ s. It is obvious that when the moving time difference Δt increases, the temporal correlation decrease gradually [37]. Furthermore, we investigate the temporal ACFs of the proposed channel model for some specific moving directions of the UAV. Note that when the UAV moves away from the azimuth plane, i.e., $\varphi_T = 0$ and $\gamma_T = \pi/2$, the height of the UAV increases slowly. In this case, the temporal correlations gradually decrease as the time t varies from 1 s to 5 s. When the UAV moves towards the azimuth plane, i.e., $\varphi_T = 0$ and $\gamma_T = -\pi/2$, the correlations increase slowly as the time t increases. These results fit the measurements in [38] very well, which also demonstrate that the temporal autocorrelations gradually decrease as the propagation distance between the transmitter and receiver increases. In addition, we notice that when the moving time t is 1 s, the differences between the above two cases are insignificant. The aforementioned simulation results agree with the conclusions in [16], thereby validating the accuracy of the above analysis and derivations.

C. Doppler PSDs

Measurements in [39] have demonstrated that the motion of the transmitter and receiver lead to perturbations of Doppler spectrum in wireless channels. In light of this, we investigate the Doppler PSDs of the proposed channel model for the case that $D_0 = 20$ m and the case that $D_0 = 100$ m in Fig. 8, which respectively correspond to the relatively small and large distances between the horizontal distance between the center points of the UAV and MR antenna arrays. It can be observed that when the horizontal distance D_0 increases from 20 m to 100 m, the propagation delay (i.e., tap number) rises correspondingly, and hence the Doppler PSDs of the proposed model decrease gradually, which agree with the measurements in [18] very well. Here, we also note that the Doppler spectrum has different behaviors at different MR's moving time t, which agrees with the results in [40]. Furthermore, the Doppler spectrum has a dominant narrow peak at the zero frequency, which is in agreement with the theoretical simulations in [41] and the measurements in [18], verifying the correctness of the simulations and derivations in (23).

D. PDPs

Similar to the discussions in Fig. 4, we investigate the PDPs of the proposed channel model for some specific MR moving directions in Fig. 9. They are the case that the MR moves

towards the origin of the coordinate, as well as the case that the MR moves away from the origin of the coordinate. It can be observed that when the MR moves away the projection point of the UAV in the horizontal plane, i.e., $\varphi_R = 0$, the propagation path length increases slowly as the motion is ongoing. In this case, the proposed PDPs decrease gradually as the propagation delay τ increases [32]. However, when the ground receiver moves towards the projection point of the UAV in the azimuth plane, i.e., $\varphi_R = \pi$, the path length approaches to be a lower value. In this case, the proposed PDPs gradually increase as the delay τ increases. Furthermore, we study the proposed PDPs for the case that $v_R = 5$ m/s and $v_R = 20$ m/s, which correspond to the relatively small and large velocities of the MR, respectively. More specifically, it is obvious that when the velocity of the MR is 20 m/s, the proposed PDP varies more significantly as the MR's velocity is 5 m/s. It is worth noting that when the time t increases from 0 to 2 s, the PDPs increase and decrease more rapidly for the cases of $\varphi_R = \pi$ and $\varphi_R = 0$, respectively. The model can be easily fitted by the measured PDP at different moving time t. Therefore, we are able to effectively analysis and design the proposed UAV-MIMO wireless communication systems.

VI. Conclusion

In this article, we have provided a 3D MIMO channel model for A2G communications in UAV scenarios. When the horizontal distance between the centers of the UAV and MR antenna elements is known, the 3D angular parameters are estimated during which the UAV and MR are stationary. Then, we estimate the real-time AAoD/EAoD and AAoA/EAoA to capture the non-stationarity of the channel model. Numerical simulation results have shown that the MLE performance of the AAoD/EAoD and AAoA/EAoA estimations performs satisfactory as the number of sequence of samples K increases gradually. Furthermore, the proposed channel characteristics, such as the spatial CCFs, temporal ACFs, Doppler PSDs, and PDPs, are closely related to the moving velocities and directions of the UAV and MR on the ground, the horizontal distances between the transceivers, UAV's height, and so on.

It is also worth mentioning the proposed estimation algorithm for characterizing the real-time channel characteristics can be used to develop new algorithms for evaluating the performance of A2G and air-to-air (A2A) communication systems in different UAV environments, such as mountain, sea, city, etc. For example, when we conduct the channel measurements in wireless networks, machine-learning-based data processing techniques can be introduced to predict the real-time properties of communication systems.

Appendix
AAoD/EAoD and AAoA/EAoA Estimations in the Preliminary Stage

In the preliminary stage the UAV and MR are assumed to be stationary, the AAoD and EAoD of the propagation path that impinge on the ℓ-th cluster, and the AAoA and EAoA of the propagation path traveling from the ℓ-th cluster are denoted as $\alpha_{\ell,T}(0)$, $\beta_{\ell,T}(0)$, $\alpha_{\ell,R}(0)$, and $\beta_{\ell,R}(0)$, respectively; the distances from the centers of the UAV and MR to the ℓ-th cluster are denoted as $D_{\ell,T}(0)$ and $D_{\ell,R}(0)$, respectively; the distances from the p-th transmit antenna and q-th receive antenna to the ℓ-th cluster are $D_{\ell,T,p}(0)$ and $D_{\ell,R,q}(0)$, respectively. In this stage, the complex CIR can be expressed as

$$h_{pq}(0,\tau) = \omega_\ell e^{j\left(\varphi_0 - 2\pi f_c \tau_{\ell,pq}(0)\right)} \delta\big(\tau - \tau_\ell(0)\big), \qquad (25)$$

where $\tau_\ell(0) = (D_{\ell,T}(0) + D_{\ell,R}(0))/c$ denotes the propagation delay of the waves emerging from the center of the UAV to that of the MR during the initialization. Furthermore, the delay $\tau_{\ell,pq}(0)$ is the propagation time of the wave from the p-th transmit antenna to the q-th receive antenna via the ℓ-th cluster, which can be derived as (26), shown at the bottom of the page. Note that in (26), $k_p = (M_T - 2p + 1)/2$, $k_q = (M_R - 2q + 1)/2$, and the distances $D_{\ell,T}(0)$ and $D_{\ell,R}(0)$ can be respectively expressed as (27) and (28), shown at the bottom of the page, where H_0 denotes the height of the UAV, D_0 is the horizontal distance between the center points of the UAV and MR antenna arrays during the initialization. This is mainly due to the fact that the propagation delay $\tau_{\ell,pq}(0)$ can be defined as the ratio of the p-th transmit and q-th receive path lengths to the speed of light, while the closed-form expressions of the p-th transmit and q-th receive path lengths are derived based on the known distance D_0 and the height H_0.

$$\begin{aligned}\tau_{\ell,pq}(0) &= \Big(D_{\ell,T,p}(0) + D_{\ell,R,q}(0)\Big)/c \\ &= \frac{1}{c}\Bigg(\sqrt{D_{\ell,T}^2(0) + (k_p\delta_T)^2 - 2D_{\ell,T}(0)k_p\delta_T \cos\beta_{\ell,T}(0)\cos\theta_T \cos\big(\alpha_{\ell,T}(0) - \psi_T\big)} - 2D_{\ell,T}(0)k_p\delta_T \sin\beta_{\ell,T}(0)\sin\theta_T \\ &\quad + \sqrt{D_{\ell,R}^2(0) + (k_q\delta_R)^2 - 2D_{\ell,R}(0)k_q\delta_R \cos\beta_{\ell,R}(0)\cos\theta_R \cos\big(\alpha_{\ell,R}(0) - \psi_R\big) - 2D_{\ell,R}(0)k_q\delta_R \sin\beta_{\ell,R}(0)\sin\theta_R}\Bigg) \end{aligned} \qquad (26)$$

$$D_{\ell,R}(0) = \frac{H_0 \cot\beta_{\ell,T}(0)\cos\alpha_{\ell,T}(0) - D_0}{\sin\beta_{\ell,R}(0)\cot\beta_{\ell,T}(0)\cot\alpha_{\ell,T}(0) + \cos\beta_{\ell,R}(0)\cos\alpha_{\ell,R}(0)} \qquad (27)$$

$$D_{\ell,T}(0) = \frac{H_0 \cot\beta_{\ell,R}(0)\cos\alpha_{\ell,R}(0) + D_0}{\sin\beta_{\ell,T}(0)\cot\beta_{\ell,R}(0)\cot\alpha_{\ell,R}(0) + \cos\beta_{\ell,T}(0)\cos\alpha_{\ell,T}(0)} \qquad (28)$$

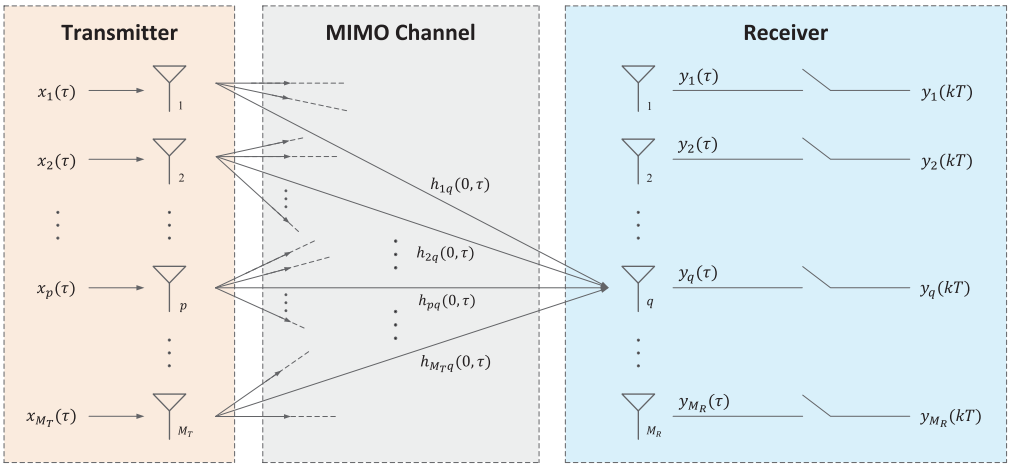

Fig. 10. Illustration of the proposed UAV MIMO communication system.

In this stage, the received signal of the q-th receive antenna element can be calculated as

$$\begin{aligned} y_q(\tau) &= \sum_{p=1}^{M_T} x_p(\tau) * h_{pq}(0,\tau) \\ &= \sum_{p=1}^{M_T} \int_{-\infty}^{\infty} h_{\ell,pq}(0)\delta\big(\lambda - \tau_\ell(0)\big) x_p(\tau-\lambda) d\lambda \\ &= \sum_{p=1}^{M_T} h_{\ell,pq}(0) x_p\big(\tau - \tau_\ell(0)\big) + n_q(\tau), \end{aligned} \tag{29}$$

where $x_p(\tau)$ denotes the p-th input signal, $*$ is the convolution operation, and $n_q(\tau)$ is the complex noise of the q-th receive antenna. As demonstrated in [42], the output of wireless communication system can be simply expressed as product of complex fading envelope and the transmitted signal. By substituting (25) into (29), we can obtain the expression of the received signal of the q-th antenna element in the proposed model as

$$y_q(\tau) = \omega_\ell e^{j\left(\varphi_0 - 2\pi f_c \tau_{\ell,pq}(0)\right)} x_p\big(\tau - \tau_\ell(0)\big) + n_q(\tau). \tag{30}$$

Based on the sampling theorem, we can convert a continuous received signal $y_q(\tau)$ to a discrete sequence of samples $\{y_q(1T), y_q(2T), \ldots, y_q(KT)\}$, where K denotes the number of sequence of samples, as illustrated in Fig. 10, with no loss of information [23]. Therefore, we can rewrite the received signal of the k-th ($k = 1, 2, \ldots, K$) sequence of the q-th receive antenna element as

$$y_q(kT) = \sum_{p=1}^{M_T} \omega_\ell e^{j\left(\varphi_0 - 2\pi f_c \tau_{\ell,pq}(0)\right)} x_p\big(kT - \tau_\ell(0)\big) + n_q(kT) \tag{31}$$

where $n_q(kT)$ denotes the complex white Gaussian noise of the k-th sequence of the q-th receive antenna, i.e., $n_q(kT) \sim \mathcal{CN}(0, \sigma^2)$. Accordingly, the received signal vector of the q-th antenna of the receive array, denoted by $\mathbf{y}_q \in \mathbb{C}^K$, can be expressed as

$$\begin{aligned} \mathbf{y}_q &= \big[y_q(1T), y_q(2T), \ldots, y_q(kT), \ldots, y_q(KT)\big]^T \\ &= \underbrace{\sum_{p=1}^{M_T} \omega_\ell e^{j\left(\varphi_0 - 2\pi f_c \tau_{\ell,pq}(0)\right)} \begin{bmatrix} x_p\big(1\ T - \tau_\ell(0)\big) \\ x_p\big(2\ T - \tau_\ell(0)\big) \\ \vdots \\ x_p\big(kT - \tau_\ell(0)\big) \\ \vdots \\ x_p\big(KT - \tau_\ell(0)\big) \end{bmatrix}}_{\mathbf{m}_q} \\ &\quad + \underbrace{\begin{bmatrix} n_q(1T) \\ n_q(2T) \\ \vdots \\ n_q(kT) \\ \vdots \\ n_q(KT) \end{bmatrix}}_{\mathbf{n}_q}, \end{aligned} \tag{32}$$

where $[\cdot]^T$ denotes the transpose operation. Subsequently, the received signal vector of the proposed communication system, denoted as $\mathbf{y} \in \mathbb{C}^{M_R K}$, can be expressed as

$$\begin{aligned} \mathbf{y} &= \big[\mathbf{y}_1, \mathbf{y}_2, \ldots, \mathbf{y}_q, \ldots, \mathbf{y}_{M_R}\big]^T \\ &= \mathbf{m} + \mathbf{n}, \end{aligned} \tag{33}$$

where $\mathbf{m} = \big[\mathbf{m}_1, \mathbf{m}_2, \ldots, \mathbf{m}_q, \ldots, \mathbf{m}_{M_R}\big]^T$ and $\mathbf{n} = \big[\mathbf{n}_1, \mathbf{n}_2, \ldots, \mathbf{n}_q, \ldots, \mathbf{n}_{M_R}\big]^T$. Here, let us define $\mathbf{n} = \mathbf{n}_r + j\mathbf{n}_i$ as the $M_R K$ dimensional complex white Gaussian noise vector, where $\mathbf{n}_r = Re[\mathbf{n}]$ denotes the real part and $\mathbf{n}_i = Im[\mathbf{n}]$ is the imaginary part. Let us assume that the elements in $\mathbf{n}$ are independent and identically distributed (i.i.d), i.e., $\mathbf{n} \sim \mathcal{CN}(\mathbf{0}, \sigma^2 \mathbf{I}_{M_R K})$, where $\mathbf{I}_{M_R K}$ denote an identity matrix. To reduce the computational complexity of the AAoD/EAoD and AAoA/EAoA estimation algorithm, it is an effective method of converting the complex arithmetic based on the Euler's theorem [24]; hence, we define the vector $\mathbf{x}$ as the combination of the real parts of the $\mathbf{m}$ and $\mathbf{n}$, while $\mathbf{z}$ as

the combination of the imaginary parts of the **m** and **n**. Then, the equation (33) can be rewritten as

$$\mathbf{y} = \mathbf{x} + j\mathbf{z} = \begin{bmatrix} \mathbf{x}_1 \\ \mathbf{x}_2 \\ \vdots \\ \mathbf{x}_q \\ \vdots \\ \mathbf{x}_{M_R} \end{bmatrix} + j \begin{bmatrix} \mathbf{z}_1 \\ \mathbf{z}_2 \\ \vdots \\ \mathbf{z}_q \\ \vdots \\ \mathbf{z}_{M_R} \end{bmatrix}, \tag{34}$$

where $\mathbf{x}_q$ and $\mathbf{z}_q$ can be expressed as (35) and (36), as shown at the bottom of the page.

Let us assume that $\mathbf{y} \sim \mathcal{CN}(\boldsymbol{\mu}, \sigma^2 \mathbf{I}_{M_R K})$, with $\boldsymbol{\mu} = \boldsymbol{\mu}_x + j\boldsymbol{\mu}_z$ representing the $M_R K$ mean element. Here, let us define $\mu_{x,q,k}$ and $\mu_{z,q,k}$ as the mean values of the k-th sequence of the vectors $\mathbf{x}_q$ and $\mathbf{z}_q$, respectively, i.e.,

$$\mu_{x,q,k} = \sum_{p=1}^{M_T} \omega_\ell x_p\big(kT - \tau_\ell(0)\big) \cos\big(\varphi_0 - 2\pi f_c \tau_{\ell,pq}(0)\big), \tag{37}$$

$$\mu_{z,q,k} = \sum_{p=1}^{M_T} \omega_\ell x_p\big(kT - \tau_\ell(0)\big) \sin\big(\varphi_0 - 2\pi f_c \tau_{\ell,pq}(0)\big). \tag{38}$$

Assume that the elements in **y** are i.i.d; hence, we can obtain the probability density function (PDF) for the complex normal distribution as [42]

$$f(\mathbf{y}) = \frac{1}{\pi^{M_R \times K} \sqrt{\det(\boldsymbol{\Gamma}) \det(\overline{\boldsymbol{\Gamma}})}} \exp\Bigg\{ -\frac{1}{2} \times \Big[(\overline{\mathbf{y}} - \overline{\boldsymbol{\mu}})^T (\mathbf{y} - \boldsymbol{\mu})^T \Big] \begin{bmatrix} \boldsymbol{\Gamma} & \mathbf{0} \\ \mathbf{0} & \overline{\boldsymbol{\Gamma}} \end{bmatrix}^{-1} \begin{bmatrix} \mathbf{y} - \boldsymbol{\mu} \\ \overline{\mathbf{y}} - \overline{\boldsymbol{\mu}} \end{bmatrix} \Bigg\}. \tag{39}$$

It is worth mentioning that the statistics of the proposed complex Gaussian random vector **y** are completely determined by the covariance matrix $\boldsymbol{\Gamma}$ and $\overline{\boldsymbol{\Gamma}}$, i.e., $\boldsymbol{\Gamma} = \overline{\boldsymbol{\Gamma}} = \sigma^2 \mathbf{I}_{M_R \times K}$. Then, the PDF in (39) can be derived as

$$f(\mathbf{y}) = \frac{1}{\big(\pi\sigma^2\big)^{M_R \times K}} \times \exp\Bigg\{ -\frac{1}{\sigma^2} \times \sum_{q=1}^{M_R} \sum_{k=1}^{K} \Bigg(\Big[\overline{y_q(kT)} - \big(\mu_{x,q,k} - j\mu_{z,q,k}\big) \Big] \times \Big[y_q(kT) - \big(\mu_{x,q,k} + j\mu_{z,q,k}\big) \Big] \Bigg) \Bigg\}. \tag{40}$$

By substituting (37) and (38) into (40), we can obtain

$$\begin{aligned} f(\mathbf{y}) &= \frac{1}{\big(\pi\sigma^2\big)^{M_R K}} \times \exp\Bigg\{ -\frac{1}{\sigma^2} \\ &\times \sum_{q=1}^{M_R} \sum_{k=1}^{K} \Bigg(\overline{y_q(kT)} y_q(kT) - \big(\overline{y_q(kT)} + y_q(kT)\big) \\ &\times \sum_{p=1}^{M_T} \omega_\ell x_p\big(kT - \tau_\ell(0)\big) \cos\big(\varphi_0 - 2\pi f_c \tau_{\ell,pq}(0)\big) \\ &+ j\big(\overline{y_q(kT)} - y_q(kT)\big) \\ &\times \sum_{p=1}^{M_T} \omega_\ell x_p\big(kT - \tau_\ell(0)\big) \sin\big(\varphi_0 - 2\pi f_c \tau_{\ell,pq}(0)\big) \\ &+ \Big[\sum_{p=1}^{M_T} \omega_\ell x_p\big(kT - \tau_\ell(0)\big) \cos\big(\varphi_0 - 2\pi f_c \tau_{\ell,pq}(0)\big) \Big]^2 \\ &+ \Big[\sum_{p=1}^{M_T} \omega_\ell x_p\big(kT - \tau_\ell(0)\big) \sin\big(\varphi_0 - 2\pi f_c \tau_{\ell,pq}(0)\big) \Big]^2 \Bigg) \Bigg\}. \end{aligned} \tag{41}$$

It is also worth mentioning that the $\overline{y_q(kT)} - y_q(kT)$ is a complex variable; hence, the term $j\big(\overline{y_q(kT)} - y_q(kT)\big)$

$$\mathbf{x}_q = \begin{bmatrix} \sum_{p=1}^{M_T} \omega_\ell x_p\big(1\ T - \tau_\ell(0)\big) \cos\big(\varphi_0 - 2\pi f_c \tau_{\ell,pq}(0)\big) + n_{r,q}(1T) \\ \sum_{p=1}^{M_T} \omega_\ell x_p\big(2\ T - \tau_\ell(0)\big) \cos\big(\varphi_0 - 2\pi f_c \tau_{\ell,pq}(0)\big) + n_{r,q}(2T) \\ \vdots \\ \sum_{p=1}^{M_T} \omega_\ell x_p\big(kT - \tau_\ell(0)\big) \cos\big(\varphi_0 - 2\pi f_c \tau_{\ell,pq}(0)\big) + n_{r,q}(kT) \\ \vdots \\ \sum_{p=1}^{M_T} \omega_\ell x_p\big(KT - \tau_\ell(0)\big) \cos\big(\varphi_0 - 2\pi f_c \tau_{\ell,pq}(0)\big) + n_{r,q}(KT) \end{bmatrix} \tag{35}$$

$$\mathbf{z}_q = \begin{bmatrix} \sum_{p=1}^{M_T} \omega_\ell x_p\big(1\ T - \tau_\ell(0)\big) \sin\big(\varphi_0 - 2\pi f_c \tau_{\ell,pq}(0)\big) + n_{i,q}(1T) \\ \sum_{p=1}^{M_T} \omega_\ell x_p\big(2\ T - \tau_\ell(0)\big) \sin\big(\varphi_0 - 2\pi f_c \tau_{\ell,pq}(0)\big) + n_{i,q}(2T) \\ \vdots \\ \sum_{p=1}^{M_T} \omega_\ell x_p\big(kT - \tau_\ell(0)\big) \sin\big(\varphi_0 - 2\pi f_c \tau_{\ell,pq}(0)\big) + n_{i,q}(kT) \\ \vdots \\ \sum_{p=1}^{M_T} \omega_\ell x_p\big(KT - \tau_\ell(0)\big) \sin\big(\varphi_0 - 2\pi f_c \tau_{\ell,pq}(0)\big) + n_{i,q}(KT) \end{bmatrix} \tag{36}$$

is not complex. In light of this, the expression of $f(\mathbf{y})$ is non-complex. Next, if we consider the natural Logarithm of the PDF, the function in (41) can be rewritten as

$$\begin{aligned}
&\ln f\big(\mathbf{y}\big) \\
&= -(M_R K)\ln(\pi\sigma^2) - \frac{1}{\sigma^2} \\
&\quad \times \sum_{q=1}^{M_R}\sum_{k=1}^{K}\Bigg(\overline{y_q(kT)}y_q(kT) - \big(\overline{y_q(kT)} + y_q(kT)\big) \\
&\quad \times \sum_{p=1}^{M_T}\omega_\ell x_p\big(kT-\tau_\ell(0)\big)\cos\big(\varphi_0 - 2\pi f_c\tau_{\ell,pq}(0)\big) \\
&\quad - j\big(\overline{y_q(kT)} - y_q(kT)\big) \\
&\quad \times \sum_{p=1}^{M_T}\omega_\ell x_p\big(kT-\tau_\ell(0)\big)\sin\big(\varphi_0 - 2\pi f_c\tau_{\ell,pq}(0)\big) \\
&\quad + \Bigg[\sum_{p=1}^{M_T}\omega_\ell x_p\big(kT-\tau_\ell(0)\big)\cos\big(\varphi_0 - 2\pi f_c\tau_{\ell,pq}(0)\big)\Bigg]^2 \\
&\quad + \Bigg[\sum_{p=1}^{M_T}\omega_\ell x_p\big(kT-\tau_\ell(0)\big)\sin\big(\varphi_0 - 2\pi f_c\tau_{\ell,pq}(0)\big)\Bigg]^2\Bigg).
\end{aligned} \tag{42}$$

Let us define $\mathbf{\Theta} = [\alpha_{\ell,T}(0), \beta_{\ell,T}(0), \alpha_{\ell,R}(0), \beta_{\ell,R}(0)]^T$. After optimization with respect to $\mathbf{\Theta}$, the Maximum Likelihood Estimate (MLE) can be expressed as [42]

$$\hat{\mathbf{\Theta}} = \arg\max_{\mathbf{\Theta}} \ln f\big(\mathbf{y}\big). \tag{43}$$

In order to accurately estimate the angular parameters $\hat{\alpha}_{\ell,T}(0)$, $\hat{\beta}_{\ell,T}(0)$, $\hat{\alpha}_{\ell,R}(0)$, and $\hat{\beta}_{\ell,R}(0)$ in the preliminary stage, we can adopt many classic solutions, such as the Newton-Raphson method and grid search method [43]. Then, the propagation path lengths from the centers of the UAV and MR to the cluster, i.e., $\hat{D}_{\ell,T}(0)$ and $\hat{D}_{\ell,R}(0)$, can be estimated by substituting the above estimated initial angular parameters into (27) and (28), respectively.

REFERENCES

[1] L. Gupta, R. Jain, and G. Vaszkun, "Survey of important issues in UAV communication networks," *IEEE Commun. Surveys Tuts.*, vol. 18, no. 2, pp. 1123–1152, 2nd Quart., 2016.

[2] H. Chang, J. Bian, C.-X. Wang, Z. Bai, W. Zhou, and E.-H.-M. Aggoune, "A 3D non-stationary wideband GBSM for low-altitude UAV-to-ground V2 V MIMO channels," *IEEE Access*, vol. 7, pp. 70719–70732, 2019.

[3] S. Wu, C.-X. Wang, E.-H.-M. Aggoune, M. M. Alwakeel, and X. You, "A general 3-D non-stationary 5G wireless channel model," *IEEE Trans. Commun.*, vol. 66, no. 7, pp. 3065–3078, Jul. 2018.

[4] C.-X. Wang, J. Bian, J. Sun, W. Zhang, and M. Zhang, "A survey of 5G channel measurements and models," *IEEE Commun. Surveys Tuts.*, vol. 20, no. 4, pp. 3142–3168, 4th Quart., 2018.

[5] H. Jiang, Z. Zhang, and G. Gui, "Three-dimensional non-stationary wideband geometry-based UAV channel model for A2G communication environments," *IEEE Access*, vol. 7, pp. 26116–26122, 2019.

[6] C.-x. Wang, X. Cheng, and D. Laurenson, "Vehicle-to-vehicle channel modeling and measurements: Recent advances and future challenges," *IEEE Commun. Mag.*, vol. 47, no. 11, pp. 96–103, Nov. 2009.

[7] H. Jiang, Z. Zhang, J. Dang, and L. Wu, "A novel 3-D massive MIMO channel model for vehicle-to-vehicle communication environments," *IEEE Trans. Commun.*, vol. 66, no. 1, pp. 79–90, Jan. 2018.

[8] X. Liu *et al.*, "Transceiver design and multihop D2D for UAV IoT coverage in disasters," *IEEE Internet Things J.*, vol. 6, no. 2, pp. 1803–1815, Apr. 2019.

[9] J. Liu, Y. Shi, Z. M. Fadlullah, and N. Kato, "Space-air-ground integrated network: A survey," *IEEE Commun. Surveys Tuts.*, vol. 20, no. 4, pp. 2714–2741, 4th Quart., 2018.

[10] J. Zhang, C. Pan, F. Pei, G. Liu, and X. Cheng, "Three-dimensional fading channel models: A survey of elevation angle research," *IEEE Commun. Mag.*, vol. 52, no. 6, pp. 218–226, Jun. 2014.

[11] X. Gao, Z. Chen, and Y. Hu, "Analysis of unmanned aerial vehicle MIMO channel capacity based on aircraft attitude," *WSEAS Trans. Inf. Sci. Appl.*, vol. 10, no. 2, pp. 58–67, Feb. 2013.

[12] L. Zeng, X. Cheng, C.-X. Wang, and X. Yin, "A 3D geometry-based stochastic channel model for UAV-MIMO channels," in *Proc. IEEE WCNC*, San Francisco, CA, USA, Mar. 2017, pp. 1–5.

[13] K. Jin, X. Cheng, X. Ge, and X. Yin, "Three dimensional modeling and space-time correlation for UAV channels," in *Proc. IEEE 85th Veh. Technol. Conf. (VTC Spring)*, Sydney, NSW, Australia, Jun. 2017, pp. 1–5.

[14] K. Jiang *et al.*, "A geometry-based 3D non-stationary UAV-MIMO channel model allowing 3D arbitrary trajectories," in *Proc. IEEE WCNC*, Hangzhou, China, Oct. 2018, pp. 1–6.

[15] H. Jiang, Z. Zhang, L. Wu, and J. Dang, "Three-dimensional geometry-based UAV-MIMO channel modeling for A2G communication environments," *IEEE Commun. Lett.*, vol. 22, no. 7, pp. 1438–1441, Jul. 2018.

[16] X. Cheng and Y. Li, "A 3-D geometry-based stochastic model for UAV-MIMO wideband nonstationary channels," *IEEE Internet Things J.*, vol. 6, no. 2, pp. 1654–1662, Apr. 2019.

[17] X. Zhang and X. Cheng, "Three-dimensional non-stationary geometry-based stochastic model for UAV-MIMO Ricean fading channels," *IET Commun.*, vol. 13, no. 16, pp. 2617–2627, Oct. 2019.

[18] Z. Huang, X. Zhang, and X. Cheng, "Non-geometrical stochastic model for non-stationary wideband vehicular communication channels," *IET Commun.*, vol. 14, no. 1, pp. 54–62, Jan. 2020.

[19] Y. Li *et al.*, "Cluster-based nonstationary channel modeling for vehicle-to-vehicle communications," *IEEE Antennas Wireless Propag. Lett.*, vol. 16, pp. 1419–1422, 2017.

[20] S. Wu, C.-X. Wang, E.-H.-M. Aggoune, M. M. Alwakeel, and Y. He, "A non-stationary 3-D wideband twin-cluster model for 5G massive MIMO channels," *IEEE J. Sel. Areas Commun.*, vol. 32, no. 6, pp. 1207–1218, Jun. 2014.

[21] A. Ghazal *et al.*, "A non-stationary IMT-advanced MIMO channel model for high-mobility wireless communication systems," *IEEE Trans. Wireless Commun.*, vol. 16, no. 4, pp. 2057–2068, Apr. 2017.

[22] W. Zeng, J. Zhang, K. P. Peppas, B. Ar, and Z. Zhong, "UAV-aided wireless information and power transmission for high-speed train communications," in *Proc. IEEE ITSC*, Maui, HI, USA, Nov. 2018, pp. 3409–3414.

[23] C. Xiao, J. Wu, S.-Y. Leong, Y. R. Zheng, and K. B. Letaief, "A discrete-time model for triply selective MIMO Rayleigh fading channels," *IEEE Trans. Wireless Commun.*, vol. 3, no. 5, pp. 1678–1688, Sep. 2004.

[24] C. Xiao, Y. Zheng, and N. Beaulieu, "Novel sum-of-sinusoids simulation models for Rayleigh and Rician fading channels," *IEEE Trans. Wireless Commun.*, vol. 5, no. 12, pp. 3667–3679, Dec. 2006.

[25] B. Liu, G. Gui, S. Matsushita, and L. Xu, "Dimension-reduced direction-of-arrival estimation based on $\ell_{2,1}$ -norm penalty," *IEEE Access*, vol. 6, pp. 44433–44444, 2018.

[26] H. Huang, J. Yang, H. Huang, Y. Song, and G. Gui, "Deep learning for super-resolution channel estimation and DOA estimation based massive MIMO system," *IEEE Trans. Veh. Technol.*, vol. 67, no. 9, pp. 8549–8560, Sep. 2018.

[27] C.-Y. Chen and W.-R. Wu, "Joint AoD, AoA, and channel estimation for MIMO-OFDM systems," *IEEE Trans. Veh. Technol.*, vol. 67, no. 7, pp. 5806–5820, Jul. 2018.

[28] Q. Qin, L. Gui, P. Cheng, and B. Gong, "Time-varying channel estimation for millimeter wave multiuser MIMO systems," *IEEE Trans. Veh. Technol.*, vol. 67, no. 10, pp. 9435–9448, Oct. 2018.

[29] O. Ozdogan, E. Bjornson, and J. Zhang, "Downlink performance of cell-free massive MIMO with Rician fading and phase shifts," in *Proc. IEEE SPAWC*, Cannes, France, Jul. 2019, pp. 1–5.

[30] H. Jiang, Z. Zhang, L. Wu, J. Dang, and G. Gui, "A 3-D non-stationary wideband geometry-based channel model for MIMO vehicle-to-vehicle communications in tunnel environments," *IEEE Trans. Veh. Technol.*, vol. 68, no. 7, pp. 6257–6271, Jul. 2019.

[31] X. Cheng, Q. Yao, M. Wen, C.-X. Wang, L.-Y. Song, and B.-L. Jiao, "Wideband channel modeling and intercarrier interference cancellation for vehicle-to-vehicle communication systems," *IEEE J. Sel. Areas Commun.*, vol. 31, no. 9, pp. 434–448, Sep. 2013.

[32] Y. Yuan, C.-X. Wang, Y. He, M. M. Alwakeel, and E.-H.-M. Aggoune, "3D wideband non-stationary geometry-based stochastic models for non-isotropic MIMO vehicle-to-vehicle channels," *IEEE Trans. Wireless Commun.*, vol. 14, no. 12, pp. 6883–6895, Dec. 2015.

[33] C. F. Lopez and C.-X. Wang, "Novel 3-D non-stationary wideband models for massive MIMO channels," *IEEE Trans. Wireless Commun.*, vol. 17, no. 5, pp. 2893–2905, May 2018.

[34] M. Patzold, *Mobile Radio Channels*, 2nd ed. West Sussex, U.K.: Wiley, 2012.

[35] D. Zhu, J. Choi, and R. W. Heath, Jr., "Auxiliary beam pair enabled AoD and AoA estimation in closed-loop large-scale millimeter-wave MIMO systems," *IEEE Trans. Wireless Commun.*, vol. 16, no. 7, pp. 4770–4785, Jul. 2017.

[36] S. Payami and F. Tufvesson, "Channel measurements and analysis for very large array systems at 2.6 GHz," in *Proc. EUCAP*, Prague, Czech Republic, Mar. 2012, pp. 433–437.

[37] A. Ghazal, C.-X. Wang, B. Ai, D. Yuan, and H. Haas, "A non-stationary wideband MIMO channel model for high-mobility intelligent transportation systems," *IEEE Trans. Intell. Transp. Syst.*, vol. 16, no. 2, pp. 885–897, Apr. 2015.

[38] M. Simunek, F. P. Fontan, and P. Pechac, "The UAV low elevation propagation channel in urban areas: Statistical analysis and time-series generator," *IEEE Trans. Antennas Propag.*, vol. 61, no. 7, pp. 3850–3858, Jul. 2013.

[39] J. B. Andersen, J. O. Nielsen, G. F. Pedersen, G. Bauch, and G. Dietl, "Doppler spectrum from moving scatterers in a random environment," *IEEE Trans. Wireless Commun.*, vol. 8, no. 6, pp. 3270–3276, Jun. 2009.

[40] J. Bian *et al.*, "A WINNER+ based 3-D non-stationary wideband MIMO channel model," *IEEE Trans. Wireless Commun.*, vol. 17, no. 3, pp. 1755–1767, Mar. 2018.

[41] A. G. Zajic, "Impact of moving scatterers on vehicle-to-vehicle narrowband channel characteristics," *IEEE Trans. Veh. Technol.*, vol. 63, no. 7, pp. 3094–3106, Sep. 2014.

[42] M. S. Kay, *Fundamentals of Statistical Signal Processing: Estimation Theory*, vol. 1. Upper Saddle River, NJ, USA: Prentice-Hall, 1993.

[43] D. Ciuonzo and P. S. Rossi, "Quantizer design for generalized locally optimum detectors in wireless sensor networks," *IEEE Wireless Commun. Lett.*, vol. 7, no. 2, pp. 162–165, Apr. 2018.

Hao Jiang (Member, IEEE) received the B.S. and M.S. degrees in electrical and information engineering from the Nanjing University of Information Science and Technology, Nanjing, China, in 2012 and 2015, respectively, and the Ph.D. degree from Southeast University, Nanjing, in 2019. From 2017 to 2018, he was a Visiting Student with the Department of Electrical Engineering, Columbia University, New York City, NY, USA. Since April 2019, he has been a Professor with the School of Information Science and Engineering, Nanjing University of Information Science and Technology. His current research interests are in the general area of wireless channel measurements and modeling, B5G wireless communication networks, signal processing, machine learning, and AI-driven technologies.

Zaichen Zhang (Senior Member, IEEE) was born in Nanjing, China, in 1975. He received the B.S. and M.S. degrees in electrical and information engineering from Southeast University, Nanjing, China, in 1996 and 1999, respectively, and the Ph.D. degree in electrical and electronic engineering from The University of Hong Kong, Hong Kong, in 2002. From 2002 to 2004, he was a Post-Doctoral Fellow with the National Mobile Communications Research Laboratory, Southeast University, China. He joined the School of Information Science and Engineering, Southeast University, in 2004, where he is currently a Professor. He has authored or coauthored more than 200 articles and issued 50 patents. His current research interests include 6G wireless systems, optical wireless communication technologies, and quantum information technologies.

Cheng-Xiang Wang (Fellow, IEEE) received the B.Sc. and M.Eng. degrees in communication and information systems from Shandong University, China, in 1997 and 2000, respectively, and the Ph.D. degree in wireless communications from Aalborg University, Denmark, in 2004.

He was a Research Assistant with the Hamburg University of Technology, Hamburg, Germany, from 2000 to 2001, a Research Fellow with the University of Agder, Grimstad, Norway, from 2001 to 2005, and a Visiting Researcher with Siemens AG-Mobile Phones, Munich, Germany, in 2004. He has been with Heriot-Watt University, Edinburgh, U.K., since 2005, where he was promoted to a Professor in wireless communications in 2011. In 2018, he joined Southeast University, Nanjing, China, as a Professor. He is also a part-time Professor with the Purple Mountain Laboratories, Nanjing. He has coauthored four books, two book chapters, and more than 390 journal and conference papers, including more than 130 articles published in various IEEE journals/magazines and 23 ESI Highly Cited Papers. He has also delivered 20 invited Keynote Speeches/Talks and seven tutorials in international conferences. His current research interests include wireless channel measurements and modeling, B5G wireless communication networks, and applying artificial intelligence to wireless communication networks.

Dr. Wang is a fellow of the IET, an IEEE Communications Society Distinguished Lecturer in 2019 and 2020, and a Highly Cited Researcher recognized by Clarivate Analytics from 2017 to 2019. He is currently an Executive Editorial Committee (EEC) Member of IEEE TRANSACTIONS ON WIRELESS COMMUNICATIONS. He has served as a Technical Program Committee (TPC) Member, the TPC Chair, and the General Chair for more than 80 international conferences. He has served as an Editor for nine international journals, including IEEE TRANSACTIONS ON WIRELESS COMMUNICATIONS from 2007 to 2009, IEEE TRANSACTIONS ON VEHICULAR TECHNOLOGY from 2011 to 2017, and IEEE TRANSACTIONS ON COMMUNICATIONS from 2015 to 2017. He was a Guest Editor of IEEE JOURNAL ON SELECTED AREAS IN COMMUNICATIONS, Special Issue on *Vehicular Communications and Networks* (Lead Guest Editor), Special Issue on *Spectrum and Energy Efficient Design of Wireless Communication Networks*, and Special Issue on *Airborne Communication Networks*. He was also a Guest Editor of IEEE TRANSACTIONS ON BIG DATA, Special Issue on *Wireless Big Data*, and IEEE TRANSACTIONS ON COGNITIVE COMMUNICATIONS AND NETWORKING, Special Issue on *Intelligent Resource Management for 5G and Beyond*. He was a recipient of 11 best paper awards from IEEE GLOBECOM 2010, IEEE ICCT 2011, ITST 2012, IEEE VTC 2013-Spring, IWCMC 2015, IWCMC 2016, IEEE/CIC ICCC 2016, WPMC 2016, WOCC 2019, and IWCMC 2020.

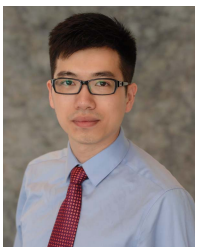

Jiangfan Zhang (Member, IEEE) received the B.Eng. degree in communication engineering from the Huazhong University of Science and Technology, Wuhan, China, in 2008, the M.Eng. degree in information and communication engineering from Zhejiang University, Hangzhou, China, 2011, and the Ph.D. degree in electrical engineering from Lehigh University, Bethlehem, PA, USA, in 2016.

From 2016 to 2018, he was a Post-Doctoral Research Scientist with the Department of Electrical Engineering, Columbia University, New York, NY, USA. Since 2018, he has been with the Department of Electrical and Computer Engineering, Missouri University of Science and Technology, Rolla, MO, USA, where he is currently an Assistant Professor. His research interests include signal processing, machine learning, and their applications to cybersecurity, cyber-physical systems, Internet of Things networks, smart grid, and sonar processing.

Dr. Zhang was a recipient of the Dean's Doctoral Student Assistantship, Gotshall Fellowship, and a P. C. Rossin Doctoral Fellow at Lehigh University.

Jian Dang (Member, IEEE) received the B.S. degree in information engineering and the Ph.D. degree in information and communications engineering from Southeast University, Nanjing, China, in July 2007 and September 2013, respectively. From September 2010 to March 2012, he was with the Department of Electrical and Computer Engineering, University of Florida, USA, as a Visiting Scholar. Since September 2013, he has been with the National Mobile Communications Research Laboratory, Southeast University. He is currently an Associate Professor. His research interests include signal processing in wireless communications and optical mobile communications.

Liang Wu (Member, IEEE) received the B.S., M.S., and Ph.D. degrees from the School of Information Science and Engineering, Southeast University, Nanjing, China, in 2007, 2010, and 2013, respectively. From September 2011 to March 2013, he was with the School of Electrical Engineering and Computer Science, Oregon State University, Corvallis, OR, USA, as a Visiting Ph.D. Student. In September 2013, he joined the National Mobile Communications Research Laboratory, Southeast University. He is currently an Associate Professor. His research interests include optical wireless communications, multiple input and multiple output technology, interference alignment, and wireless indoor localization.

Hongming Zhang (Member, IEEE) received the B.Eng. degree (Hons.) in telecommunications from the Nanjing University of Aeronautics and Astronautics (NUAA) and the City University of London in 2011, and the M.Sc. and Ph.D. degrees in wireless communications from the University of Southampton in 2012 and 2017, respectively. From 2017 to 2018, he was with the Department of Electrical Engineering, Columbia University, New York, NY, USA. He is currently an Assistant Professor with the Department of Software Engineering, Beijing University of Posts and Telecommunications, Beijing, China. His research interests include wireless communications, heterogeneous network performance analysis and optimization, and machine learning.